NANO LETTERS

Letter

pubs.acs.org/NanoLett

Multifold Enhancement of Third-Harmonic Generation in Dielectric Nanoparticles Driven by Magnetic Fano Resonances

Alexander S. Shorokhov,[†] Elizaveta V. Melik-Gaykazyan,[†] Daria A. Smirnova,[‡] Ben Hopkins,[‡] Katie E. Chong,[‡] Duk-Yong Choi,[§] Maxim R. Shcherbakov,[†] Andrey E. Miroshnichenko,[‡] Dragomir N. Neshev,[‡] Andrey A. Fedyanin,[†] and Yuri S. Kivshar*[,‡]

[†]Faculty of Physics, Lomonosov Moscow State University, Moscow 119991, Russia

[‡]Nonlinear Physics Centre, Research School of Physics and Engineering, The Australian National University, Canberra, Australian Capital Territory 2601, Australia

[§]Laser Physics Centre, Research School of Physics and Engineering, The Australian National University, Canberra, Australian Capital Territory 2601, Australia

S *Supporting Information*

ABSTRACT: Strong Mie-type magnetic dipole resonances in all-dielectric nanostructures provide novel opportunities for enhancing nonlinear effects at the nanoscale due to the intense electric and magnetic fields trapped within the individual nanoparticles. Here we study third-harmonic generation from quadrumers of silicon nanodisks supporting high-quality collective modes associated with the magnetic Fano resonance. We observe nontrivial wavelength and angular dependencies of the generated harmonic signal featuring a multifold enhancement of the nonlinear response in oligomeric systems.

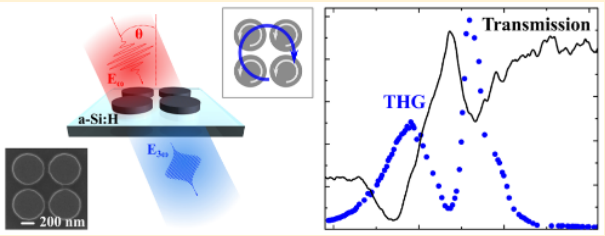

KEYWORDS: *Nonlinear optics, metamaterials, silicon photonics, third-harmonic generation, Fano resonance*

Fano resonances have been employed widely in nanophotonics due to numerous applications arising from their sharp spectral features.[1,2] These applications include solar energy harvesting,[3] biosensing,[4,5] and nonlinear optics,[6−10] to name a few. In particular, many intriguing properties of Fano resonances have been realized with metallic nanoparticles combined in small clusters often called "metamolecules" or "oligomers".[2,6,11,12] Such nanoparticle clusters exhibit the optical response uniquely defined by hybridized collective modes and their interference.[13] Plasmonic Fano resonances are usually observed through the far-field interference of the modes of the electric origin. However, the recent studies of Fano resonances in high-index dielectric nanoparticle oligomers[14−16] reveal that subwavelength metamolecules consisting of closely spaced dielectric nanoparticles can support both electric and magnetic types of the Fano resonances at optical frequencies. In a sharp contrast to many plasmonic systems, all-dielectric nanostructures offer novel capabilities of the resonant optically induced magnetic response[17−22] that can be employed for the realization of anomalous scattering signatures with the existence of *magnetic Fano resonances*.[23] Here we demonstrate experimentally, for the first time to our knowledge, that the magnetic Fano resonances may become crucially important in the multifold enhancement of nonlinear optical effects.

The study of nonlinear effects with high-index dielectric nanoparticles[9,24] is emerging as a promising alternative to plasmonic systems usually utilized for nonlinear nanophotonics,[25] due to negligible Ohmic losses and low heating in combination with multipolar radiation characteristics of both electric and magnetic nature.[26] As was already demonstrated experimentally, resonant effects accompanying light scattering in silicon nanostructures considerably increase the efficiency of the nonlinear wavelength conversion.[24] Particularly, it was established that a strong enhancement of the nonlinear response can be achieved in isolated silicon nanodisks optically pumped in the vicinity of their magnetic dipolar resonance due to the significantly enhanced local fields tightly bound within the nanodisk volume. Combining dielectric particles in oligomers may lead to the formation of collective modes with different lifetimes limited by radiative losses mainly, in a striking contrast to deeply subwavelength plasmonic analogues. Importantly, such multiresonant dielectric nanostructures can be designed to support high-quality modes of different symmetries, amplifying dramatically nonlinear optical effects.

In this Letter, we analyze the nonlinear scattering from dielectric clusters composed of four identical silicon nanodisks (see Figure 1) excited in the spectral range close to the magnetic dipole resonance of the individual disk. We show, for the first time to our knowledge, that resonant excitation of collective modes in such symmetric quadrumers results in

Received: March 24, 2016
Revised: June 23, 2016
Published: July 12, 2016

DOI: 10.1021/acs.nanolett.6b01249
Nano Lett. 2016, 16, 4857−4861

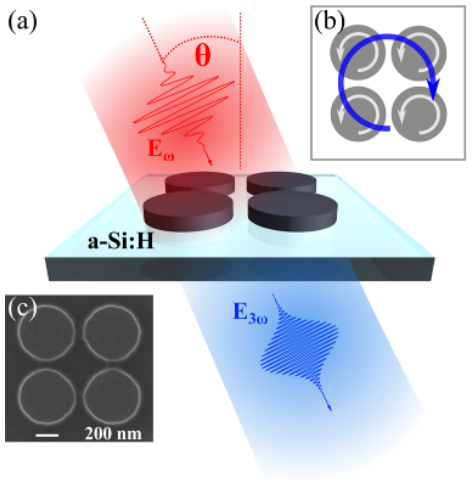

Figure 1. Schematic illustration of the resonant third-harmonic generation in silicon quadrumers. (a) The sample comprises a square array of symmetric clusters of four a-Si:H nanodisks. Quadrumers are excited by an oblique plane wave in the vicinity of the magnetic dipole resonance. (b) Origin of the magnetic Fano resonance in quadrumers—the coupled magnetic-like modes formed by out-of-plane magnetic dipoles and circulating displacement current produced by in-plane electric dipoles interfere destructively in the far-field. (c) SEM image of the sample under study.

substantial enhancement of the nonlinear response, as compared to that from both optically decoupled silicon disks and an unpatterned silicon film of the same thickness. We observe nontrivial wavelength and angular dependencies of the generated radiation, featuring a peak third-harmonic signal in the vicinity of the magnetic Fano resonance. Particularly, excitation of the magnetic collective modes in quadrumers allows for the extremely enhanced local fields within the magnetic dipolar response of the constituent disks, being beneficial for the nonlinear processes. Note here that such a mechanism for the third-harmonic generation (THG) enhancement in a single unit cell of all-dielectric metasurfaces is different from that reported recently in ref 9, where the high-quality resonance, achieved in a two-dimensional array of coupled silicon disks and bars, stems from the lattice modes based on the electromagnetic interaction between multiple unit cells.

For experimental studies, we use nanodisks made of hydrogenated amorphous silicon (a-Si:H) which are situated on a glass substrate. Silicon is chosen because of its compatibility with CMOS technology, a high refractive index being essential for sustaining magnetic dipole resonances in the required frequency range. Using a-Si:H films instead of silicon-on-insulator (SOI) wafers allows us to avoid unwanted interference inside a substrate SiO_2 layer as well as to remove the background signal from the substrate. Moreover, a-Si:H is known to possess a large cubic optical nonlinearity,[27] which makes it a promising material for nonlinear nanophotonics. We also choose nanodisks instead of any other shapes for creating quadrumer clusters because the positions of both electric and magnetic Mie resonances[28] can be easily tuned by varying the aspect ratio.

Samples are fabricated from a 100 nm a-Si:H film on a glass substrate. The a-Si:H film is grown by plasma-enhanced chemical vapor deposition (see Methods, section Sample Fabrication). We use electron-beam lithography to create a negative resist mask followed by reactive-ion etching to fabricate lattices of nanodisk quadrumers. The fabricated structure has a period of 1.64 μm in both lateral directions, and the diameter of an individual disk is 550 nm; the disk height is 100 nm, and the interparticle gap between the disks in a single quadrumer is 100 nm.

The idea of our experiment is sketched in Figure 1a. We excite nanodisks by obliquely incident intense femtosecond laser pulses with the frequency ω tuned to the spectral vicinity of magnetic dipole resonances of the individual nanoparticles. Due to a strong field localization inside the nanodisks and high nonlinear third-order susceptibility $\chi^{(3)}$ of a-Si:H, we achieve substantial third-harmonic generation from the quadrumer clusters.

In our experiment, we collect and analyze the transmitted third-harmonic signal and trace the harmonic radiation relative to the resonant linear spectrum of the quadrumer structure. A scanning electron micrograph (SEM) of the quadrumer unit cell is shown in Figure 1c. Using an optical setup based on a white light source and an IR spectrometer (see Methods, section Experimental Setup), we first measure the linear transmission spectrum, which is shown in Figure 2a by a

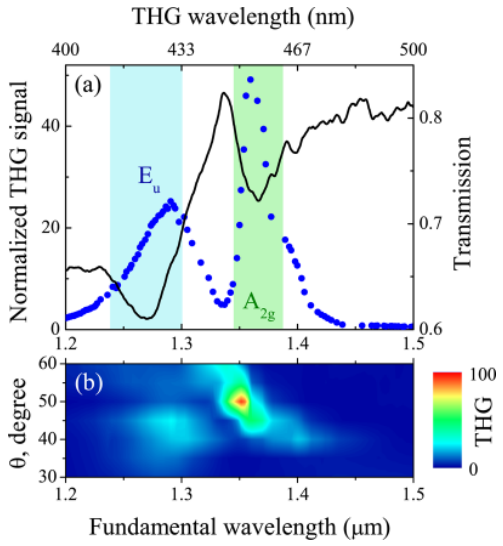

Figure 2. THG spectroscopy of quadrumers metasurfaces. (a) Experimental transmission (black line) and THG (blue dots) spectra of the sample for the incident angle of 45°. TH power plotted is normalized to the spectrum of a bare a-Si:H film with the thickness of 100 nm. The blue area indicates the position of the E_u resonance mode of the structure, while the green area indicates the position of the A_{2g} mode of the structure. (b) The measured angular dependence of the normalized THG from the a-Si:H quadrumers.

black curve. The spectrum is normalized to the that of a bare glass substrate, where the a-Si:H film is etched away. Two distinctive resonant dips are clearly seen in the experimental plot.

Next, we perform third-harmonic (TH) spectroscopy measurements. For the excitation we use the pulse train from an optical parametric oscillator (OPO) pumped by a femtosecond Ti:sapphire laser (see Methods, section Experimental Setup). It allows us to achieve high peak intensities in the pump beam for the substantial THG as well as to avoid

DOI: 10.1021/acs.nanolett.6b01249
Nano Lett. 2016, 16, 4857−4861

sample thermal damage. To neglect the role of the intrinsic $\chi^{(3)}$ dispersion of the a-Si:H and to avoid any artifacts connected with the OPO output power variations, we use an additional channel with a 100 nm a-Si:H film as a source for the reference TH signal. For each pump wavelength, THG was measured consecutively from the sample and from the a-Si:H film at the same experimental conditions. Normalizing the spectrum from the sample over the reference spectrum of the a-Si:H film, we extract the THG wavelength dependence depicted in Figure 2a with blue dots. Since in both cases we use the same a-Si:H, the normalized THG spectrum cancels out the $\chi^{(3)}$ dispersion, providing a clear indication of the magnetic resonant contributions to the nonlinear response of the structure.

To clarify the experimental results, we model both the linear and nonlinear optical responses of a-Si:H quadrumers arranged in a square lattice using the finite-element method (FEM) solver of COMSOL Multiphysics software package (see Methods, section Numerical Simulations). In agreement with the measured dependence, the calculated linear transmission spectrum displayed in Figure 3a shows a broad transmission dip and a sharp Fano-like line shape at longer wavelengths. Inhomogeneous broadening of the resonance observed in the transmittance spectrum could be caused by the finite numerical aperture of the focusing system, as well as by the inhomogeneities of the nanodisk dimentions. To reveal the nature of these features, we examine the near-field profiles at the corresponding spectral positions and assign them to different collective modes in quadrumers that can be classified according to the irreducible representations of the quadrumer's symmetry group D_{4h}, as discussed in ref 23. Specifically, we attribute the first dip centered at 1.28 μm to the predominant excitation of the E_u magnetic mode, which is essentially formed by four magnetic dipoles oppositely oriented out of the sample plane for top and bottom disks of the quadrumer (see Figure 3b and Supporting Information). The pronounced Fano dip near 1.34 μm basically originates from the destructive far-field interference of two A_{2g} (magnetic and electric) modes strongly coupled through the near-field interaction, as described in detail in ref 23. The A_{2g} magnetic mode is formed by four magnetic dipoles co-oriented out of the sample plane, while the electric mode is constructed by electric dipoles excited in the plane, which constitute a circular displacement current over the four disks (see the Supporting Information, Figure S1). Accepting the coupled dipole description, we estimate the ratio of radiative dampings for antisymmetric (E_u) and symmetric (A_{2g}) configurations of out-of-plane magnetic dipoles separated by approximately a half of the free space fundamental wavelength in our geometry. This ratio of about 4 explains the relative spectral widths of the two resonances in transmission and proves a subradiant character of the A_{2g} magnetic mode involved in the Fano interference. Under resonant conditions, this mode is driven through the coupling to the electric A_{2g} mode excited by incident radiation, which results in strong enhancement of the trapped optical near-field.

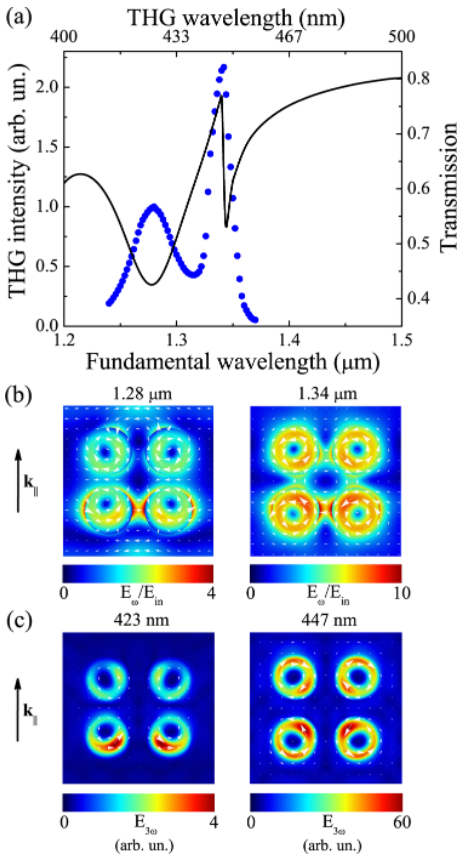

Figure 3. Theoretical results. (a) Calculated linear transmission (black curve) and TH (blue dots) spectra of the a-Si:H quadrumers array excited by an obliquely incident $s(x)$-polarized plane wave at the angle of 45°. THG power is shown normalized to the low-wavelength maximum. Simulated distributions of the electric field magnitude superimposed with field vectors near the E_u magnetic (1.28 μm) and A_{2g} magnetic Fano (1.34 μm) resonances for both fundamental (b) and third-harmonic (c) frequencies in a single quadrumer. The fields are evaluated in the horizontal xy cut-plane passing through the disk centers. Black arrows illustrate an in-plane wavevector $\mathbf{k}_{\|}$ of the incident radiation.

Importantly, both resonances are characterized by pronounced magnetic dipolar excitations in the disks and significant local field enhancement, as shown in Figure 3b, and thereby they are accompanied by a substantial increase of the third-harmonic signal, with the corresponding TH near-field profiles depicted in Figure 3c. In particular, we observe an increase of the THG in the vicinity of the magnetic E_u mode of the quadrumer up to 25 times in comparison with a bulk a-Si:H film. However, we obtain up to 50 times enhancement of the harmonic conversion when the magnetic Fano resonance of the quadrumers is excited (see Figure 2a). This is found to be consistent with the results of numerical simulations shown in Figure 3a. Remarkably, these enhancement factors outreach by a factor of 4 the enhancement that can be realized in a metasurface of equidistantly spaced nanodisks with the same filling factor of the nonlinear material as shown in calculations provided in Supporting Information, Figure S3. It is worth mentioning that the experimentally observed THG peaks are slightly spectrally shifted with respect to the transmission dips, while in calculations no shift is apparent. There are two main aspects that might be responsible for the mismatch. First, for the sake of larger intensity, in THG experiments the area illuminated by femtosecond radiation was kept much smaller than that during the linear measurements. It is therefore clear that the actual transmittance spectra of the THG-emitting quadrumers were slightly different from that obtained in transmittance measurements. Second, a possible reason for the experimentally observed spectral shift and its lack in calculations is that in our simulations no $\chi^{(3)}$ dispersion was

DOI: 10.1021/acs.nanolett.6b01249
Nano Lett. 2016, 16, 4857−4861

taken into account, whereas in silicon, a strong wavelength-dependent variation of the bulk $\chi^{(3)}$ is possible due to the onset of direct interband transitions at approximately 400 nm.

We expect that the sharpness of the magnetic Fano feature is strongly dependent on the angle of illumination.[23] With this knowledge, we perform angular spectroscopy of the THG radiation. Experimental results are presented in Figure 2b. Although the magnetic Fano resonance could be excited most effectively with a grazing incidence,[23] experimentally it is more feasible to consider angles of the incident beam in the range between 30° and 60° due to the finite dimensions of the sample. Changing the incident angle in this range, we are able to observe a significant enhancement of the nonlinear optical response from the quadrumers in the vicinity of the magnetic Fano resonance—up to 10 times larger than that at the magnetic E_u mode of the same a-Si:H nanodisks cluster, or a hundred-fold increase if compared with a nonstructured a-Si:H film. The estimated THG conversion efficiency for the quadrumers sample was up to 10^{-6}, which is 10 times larger than that in our previous studies of an array of optically decoupled silicon nanodisks.[24]

In summary, we have observed a multifold enhancement of the third-harmonic generation in dielectric quadrumers composed of silicon nanodisks, due to the Fano resonance originating from the interference of individual and collective optically induced magnetic modes. Importantly, the respective linear near-field distribution resembles a magnetic toroidal dipole mode excitation, analogous to its electric counterpart.[29,30] We expect that our findings will trigger further studies of strong optical nonlinearities in all-dielectric oligomeric and toroidal systems.

Methods. *Sample Fabrication.* The sample shown in Figure 1 was fabricated on a glass substrate using the following procedure. A layer of 100 nm hydrogenated amorphous silicon was deposited using plasma-enhanced chemical vapor deposition in the Oxford PlasmaLab System 100 under the conditions of 25 sccm SiH_4 and 475 sccm He at 250 °C for approximately 5 min. Negative tone ma-N-2403 electron beam resist (300 nm) was then spin-coated over the film, as well as a water-soluble anticharging conductive polymer (ESPACER 300Z) to avoid static charging during electron beam lithography. We exposed the resist using an electron-beam lithography system (Raith 150) and then removed the anticharging layer in deionized water. The exposed film was developed in ma-D-525 for 80 s and brought to a reactive ion etching facility (Oxford PlasmaLab System 100). The following mixture of gases was used to etch the film through the resist mask: 1.8 sccm SF_6 and 50 sccm CHF_3 at 10 mT and 500 W ICP Forward Power. To avoid systematic fabrication errors, we fabricated series of samples with different dose factors and chose one with the best parameters.

Experimental Setup. For the linear optical measurements we used a setup based on a halogen lamp light source. After passing through a collimating system and a broadband Glan polarizer, white light was focused to a sample surface by an aspheric lens with a numerical aperture of NA = 0.25. The transmitted light was collected by another lens and coupled into a multimode fiber, connected to a spectrometer. We use a Solar-LS M266 grating spectrometer equipped with a convection-cooled Hamamatsu InGaAs CCD linear array, providing subnm spectral resolution in the range from 800 to 1600 nm. Transmission spectra were obtained by normalization of the sample spectrum over the substrate spectrum, measured under the same conditions from the glass area of the sample, where the a-Si:H film was etched away.

For THG spectroscopy we used an OPO system pumped by a Coherent Chameleon Ultra II Ti:sapphire laser operated at 838 nm. The central wavelength of the pump beam was tuned in the range from 1.2 to 1.5 μm, with maximum mean power in the sample plane up to 40 mW. The s-polarized pump beam was modulated by a 1:1 chopper at a frequency of 2.1 kHz and focused by an aspheric lens with a numerical aperture of NA = 0.25 to a waist of 10 μm in diameter leading to a maximum peak intensity value of I = 5 GW/cm^2. The collecting lens placed after the sample gathered only the transmitted light; all diffracted TH beams were not detected in the experiment. The transmitted TH beam was directed to a Hamamatsu H9307 PMT module through a 5 mm set of Schott BG39 filter in order to remove the pump radiation. To improve the signal-to-noise ratio, we analyzed the voltage output of the PMT with a lock-in amplifier coupled to the optical chopper. The signal was proved to be of TH origin by checking its cubic dependence on the pump power and measuring its spectrum directly with a Solar-LS S100 concave grating wide-range spectrometer. The signal from the sample was normalized with respect to the signal from the a-Si:H 100 nm film, which was achieved under the same experimental conditions (see section Sample Fabrication).

Numerical Simulations. The electromagnetic response of the quadrumers array was calculated using finite-element method based software COMSOL Multiphysics. In our simulations, the complex dielectric permittivity of a-Si:H disks as a function of frequency was taken from the data measured with J.A. Woollam Co. Spectroscopic Ellipsometer M-2000D for the actual a-Si:H film. The refractive index of the glass substrate was set constant 1.45 over the whole spectral range of interest. Considering the array of quadrumers placed on a semi-infinite substrate in the xy plane and illuminated by the s-polarized plane wave (with E_x electric field component) at the angle of 45° from the air upper halfspace, we calculated numerically the transmission spectrum. In order to obtain the far-field optical spectra, a single unit cell of the array was modeled with the perfectly matched layer (PML) and Floquet periodic boundary conditions imposed in the vertical (along the z-axis) and both lateral directions (along the x- and y-axes), respectively. PMLs on the top and bottom of the unit cell prevent parasitic interference in the modeling. Port boundary conditions placed at the interior boundaries of the PMLs allow for both setting an excitation plane wave source and extracting the reflection and transmission characteristics in terms of scattering S-parameters. Alternatively, electric fields attained in COMSOL are evaluated at some distance away from the metasurface, and the far-field diffraction orders are differentiated by postprocessing with the use of the fast Fourier transform. The total power transmitted to the substrate is computed by integrating the outgoing power flow normalized to the power transmitted through a homogeneous air medium To calculate the TH emission from the structure, we used two coupled electromagnetic models, assuming the undepleted pump field. First, we simulated the linear scattering of the pump plane wave to retrieve the local field distribution and compute the bulk nonlinear polarization induced inside the nanodisks, $\mathbf{P}^{(3\omega)} = \chi^{(3)}[\mathbf{E}_{\mathrm{loc}}^{(\omega)}]^3$, where $\chi^{(3)}$ is the third-order susceptibility of silicon and $\mathbf{E}_{\mathrm{loc}}^{(\omega)}$ is the local complex electric field at the fundamental frequency. Second, this polarization was employed as a source for the next electromagnetic simulation at the TH frequency to obtain the generated field

DOI: 10.1021/acs.nanolett.6b01249
Nano Lett. 2016, 16, 4857−4861

and then recover the TH power flux radiated to the substrate. The simulations were carried out assuming continuous wave excitation of the infinitely extended array and did not account for a finite aperture of the pump beam and possible imperfections of the fabricated sample. In reality, these factors may lead to reducing the quality factors of the resonances. However, in the proximity of the sharp and narrow Fano feature, a finite duration of the laser pulses was taken into account by relating the excitation bandwidth and the spectral width of the Fano resonance, which effectively results in scaling down the associated peak in THG, essentially reproducing the THG wavelength dependence observed experimentally. Specifically, we calculate the time evolution of the modal amplitude analytically, similar to dynamics of a conventional oscillator and deduce the integral attenuation factor of THG compared to the monochromatic case. This procedure quantifies reducing the resonant peak in the THG spectrum and realistically reflects the experimental conditions.

ASSOCIATED CONTENT

Supporting Information

The Supporting Information is available free of charge on the ACS Publications website at DOI: 10.1021/acs.nanolett.6b01249.

Explanation of the electric and magnetic dipole coupling mechanism; results of simulations in the case of individual nanodisks; supplementary experimental data that verifies THG (PDF)

AUTHOR INFORMATION

Corresponding Author

*E-mail: ysk@internode.on.net.

Notes

The authors declare no competing financial interest.

ACKNOWLEDGMENTS

The authors are grateful to P. Banzer, M. Decker, L. Novotny, I. Staude, and N. Zheludev for useful discussions. This work was supported by the Australian Research Council, the Russian Science Foundation (Grant 14-12-01144, experimental part), and the Russian Foundation for Basic Research (Grant 16-32-00265). This work was performed in part at the ACT node of the Australian National Fabrication Facility, a company established under the National Collaborative Research Infrastructure Strategy to provide nano and micro-fabrication facilities for Australia's researchers.

REFERENCES

(1) Miroshnichenko, A. E.; Flach, S.; Kivshar, Y. S. *Rev. Mod. Phys.* **2010**, *82*, 2257−2298.

(2) Luk'yanchuk, B.; Zheludev, N. I.; Maier, S. A.; Halas, N. J.; Nordlander, P.; Giessen, H.; Chong, C. T. *Nat. Mater.* **2010**, *9*, 707−715.

(3) Wu, C.; Neuner, B.; John, J.; Milder, A.; Zollars, B.; Savoy, S.; Shvets, G. *J. Opt.* **2012**, *14*, 024005.

(4) Lahiri, B.; Khokhar, A. Z.; De La Rue, R. M.; McMeekin, S. G.; Johnson, N. P. *Opt. Express* **2009**, *17*, 1107−1115.

(5) Wu, C.; Khanikaev, A. B.; Adato, R.; Arju, N.; Yanik, A. A.; Altug, H.; Shvets, G. *Nat. Mater.* **2011**, *11*, 69−75.

(6) Thyagarajan, K.; Butet, J.; Martin, O. J. F. *Nano Lett.* **2013**, *13*, 1847−1851.

(7) Metzger, B.; Schumacher, T.; Hentschel, M.; Lippitz, M.; Giessen, H. *ACS Photonics* **2014**, *1*, 471−476.

(8) Smirnova, D. A.; Miroshnichenko, A. E.; Kivshar, Y. S.; Khanikaev, A. B. *Phys. Rev. B: Condens. Matter Mater. Phys.* **2015**, *92*, 161406.

(9) Yang, Y.; Wang, W.; Boulesbaa, A.; Kravchenko, I. I.; Briggs, D. P.; Puretzky, A.; Geohegan, D.; Valentine, J. *Nano Lett.* **2015**, *15*, 7388−7393.

(10) Liu, S.-D.; Leong, E. S. P.; Li, G.-C.; Hou, Y.; Deng, J.; Teng, J. H.; Ong, H. C.; Lei, D. Y. *ACS Nano* **2016**, *10*, 1442−1453.

(11) Shafiei, F.; Monticone, F.; Le, K. Q.; Liu, X.-X.; Hartsfield, T.; Alú, A.; Li, X. *Nat. Nanotechnol.* **2013**, *8*, 95−99.

(12) Zhang, Y.; Wen, F.; Zhen, Y.-R.; Nordlander, P.; Halas, N. J. *Proc. Natl. Acad. Sci. U. S. A.* **2013**, *110*, 9215−9219.

(13) Fan, J. A.; Wu, C.; Bao, K.; Bao, J.; Bardhan, R.; Halas, N. J.; Manoharan, V. N.; Nordlander, P.; Shvets, G.; Capasso, F. *Science* **2010**, *328*, 1135−1138.

(14) Miroshnichenko, A. E.; Kivshar, Y. S. *Nano Lett.* **2012**, *12*, 6459−6463.

(15) Hopkins, B.; Poddubny, A. N.; Miroshnichenko, A. E.; Kivshar, Y. S. *Phys. Rev. A: At., Mol., Opt. Phys.* **2013**, *88*, 053819.

(16) Chong, K. E.; Hopkins, B.; Staude, I.; Miroshnichenko, A. E.; Dominguez, J.; Decker, M.; Neshev, D. N.; Brener, I.; Kivshar, Y. S. *Small* **2014**, *10*, 1985−1990.

(17) Garcia-Etxarri, A.; Gómez-Medina, R.; Froufe-Pérez, L. S.; López, C.; Chantada, L.; Scheffold, F.; Aizpurua, J.; Nieto-Vesperinas, M.; Sáenz, J. J. *Opt. Express* **2011**, *19*, 4815−4826.

(18) Ginn, J. C.; Brener, I.; Peters, D. W.; Wendt, J. R.; Stevens, J. O.; Hines, P. F.; Basilio, L. I.; Warne, L. K.; Ihlefeld, J. F.; Clem, P. G.; Sinclair, M. B. *Phys. Rev. Lett.* **2012**, *108*, 097402.

(19) Evlyukhin, A. B.; Novikov, S. M.; Zywietz, U.; Eriksen, R. L.; Reinhardt, C.; Bozhevolnyi, S. I.; Chichkov, B. N. *Nano Lett.* **2012**, *12*, 3749−3755.

(20) Kuznetsov, A. I.; Miroshnichenko, A. E.; Fu, Y. H.; Zhang, J.; Luk'yanchuk, B. Magnetic light. *Sci. Rep.* **2012**, *2*, 492.

(21) Liu, S.; Sinclair, M. B.; Mahony, T. S.; Jun, Y. C.; Campione, S.; Ginn, J.; Bender, D. A.; Wendt, J. R.; Ihlefeld, J. F.; Clem, P. G.; Wright, J. B.; Brener, I. *Optica* **2014**, *1*, 250−256.

(22) Jahani, S.; Jacob, Z. *Nat. Nanotechnol.* **2016**, *11*, 23−36.

(23) Hopkins, B.; Filonov, D. S.; Miroshnichenko, A. E.; Monticone, F.; Alú, A.; Kivshar, Y. S. *ACS Photonics* **2015**, *2*, 724−729.

(24) Shcherbakov, M. R.; Neshev, D. N.; Hopkins, B.; Shorokhov, A. S.; Staude, I.; Melik-Gaykazyan, E. V.; Decker, M.; Ezhov, A. A.; Miroshnichenko, A. E.; Brener, I.; Fedyanin, A. A.; Kivshar, Y. S. *Nano Lett.* **2014**, *14*, 6488−6492.

(25) Kauranen, M.; Zayats, A. V. *Nat. Photonics* **2012**, *6*, 737−748.

(26) Smirnova, D. A.; Khanikaev, A. B.; Smirnov, L. A.; Kivshar, Y. S. *ACS Photonics* **2016**.10.1021/acsphotonics.6b00036

(27) Ikeda, K.; Shen, Y.; Fainman, Y. *Opt. Express* **2007**, *15*, 17761−17771.

(28) Staude, I.; Miroshnichenko, A. E.; Decker, M.; Fofang, N. T.; Liu, S.; Gonzales, E.; Dominguez, J.; Luk, T. S.; Neshev, D. N.; Brener, I.; Kivshar, Y. *ACS Nano* **2013**, *7*, 7824−7832.

(29) Basharin, A. A.; Kafesaki, M.; Economou, E. N.; Soukoulis, C. M.; Fedotov, V. A.; Savinov, V.; Zheludev, N. I. *Phys. Rev. X* **2015**, *5*, 011036.

(30) Papasimakis, N.; Fedotov, V. A.; Savinov, V.; Raybould, T. A.; Zheludev, N. I. *Nat. Mater.* **2016**, *15*, 263−271.

DOI: 10.1021/acs.nanolett.6b01249
Nano Lett. 2016, 16, 4857−4861